

# Some Features of the Landslide Mechanism of Surface Waves Generation in Real Basins

Sofia A. Beisel, Leonid B. Chubarov and Yurii I. Shokin

**Abstract** We present the results of numerical modeling of surface wave generation by the movement of submerged deformable body along the slope, which simulates the real coastal slope. The multiparametric computations are carried out within the shallow water approximation that allowed to determine the dependence of wave pattern on the depth of landslide embedding, length and thickness of the body, relative density, friction coefficient, and slope geometry. The main attention is focused on the effects resulted from the heterogeneity of depths, which simulates specifics of real water basins.

## 1 Introduction

The interest in the investigations of the landslide mechanism of surface waves generation in nearshore water areas is caused by a number of catastrophic events caused by this mechanism that had happened in the recent years in different basins of the World Ocean. The landslide mechanism of tsunami wave generation is called abnormal in contrast to the conventional seismic one. Here abnormality means inconsistency between significant tsunami wave near the shore and a weak earthquake, which is associated with the generation of this wave and actually can be only a trig-

---

Sofia A. Beisel

Institute of Computational Technologies SB RAS, Lavrentiev Ave. 6, Novosibirsk, 630090, Russia,  
e-mail: beisels@gmail.com

Leonid B. Chubarov

Institute of Computational Technologies SB RAS, Lavrentiev Ave. 6, Novosibirsk, 630090, Russia,  
e-mail: chubarov@ict.nsc.ru

Yurii I. Shokin

Institute of Computational Technologies SB RAS, Lavrentiev Ave. 6, Novosibirsk, 630090, Russia,  
e-mail: shokin@ict.nsc.ru

ger for the landslide mechanism of wave generation. The portion of such events is estimated at about 15% of registered historical tsunamis.

To solve the problem of mathematical modeling of the landslide induced wave generation, both the models of landslide motion and of the ambient fluid should be built. The known approaches to the simulation of landslides include the simulation of the motion of an absolutely rigid body [5, 7] or a set of such bodies [13], simulating a fluid flow of different density, viscosity, etc. [10], or simulating the motion of an elasticoplastic medium [4] with or without taking into account the interaction with the ambient fluid. In some situations it appears promising to simulate the phenomenon as a two-layer fluid with layers of various densities and viscosity coefficients [8]. In [7, 12, 14] it is shown that substitution of the real landslide by a model rigid body coupled with an appropriate law of motion gives an adequate description of wave processes in the wide range of such parameters as slope angle, thickness and length of the body, and its initial submergence.

The specifics of the simulation of landslide generated surface waves is that this waves are generated in the nearshore zone of a small depth, and the duration of the landslide motion is quite long and comparable with the period of the generated wave; the characteristic depth and the vertical size of the landslide are comparable as well. Therefore hydrodynamic aspects of wave processes are being investigated in the framework of approximate models of wave hydrodynamics. Earlier investigations by the authors let us estimate the capabilities of different models by comparing their results with laboratory experiments. These investigations were carried out for the simplest relief consisted of the uniform slope and the flat bottom. The conclusion [2] was that even the simplest shallow water models give an adequate qualitative description of wave regimes within the special range of problem parameters, while nonlinear-dispersive models, that take into account density non-hydrostaticity (or, what is the same, the vertical fluid motion), should be used for detailed investigations.

In previous investigations, when a landslide was represented as a rigid body, only its movement along the uniform slope was considered in the law of motion. For numerical modeling of the landslide motion along such slope [1, 6], a flat bottom was attached at some depth, and for the landslide not to enter this zone, its velocity was being decreased forcibly for the body to stop at the end of the slope. Such artificial deceleration with a jump or a break of the velocity caused stop waves or deceleration waves with significant amplitude.

In the present paper an attempt is made to model the surface waves generation by the landslide moving along the arbitrary curvilinear slope according to the motion law, that takes into account slope irregularity. In particular, the possibility of a landslide to continue its movement along the flat bottom is possible, and its deceleration results from the bottom friction and hydrodynamic drag. Such natural smooth deceleration of the landslide avoids the effects of an abrupt stop noted above.

Our main attention is focused on the comparison of results obtained on the piecewise linear and "real" curvilinear slopes. The results of computational experiments let us determine the base invariable characteristics of wave processes and the parameters, which depend on the slope form. We discuss the results of comparison

of wave regimes, generated above different bottom reliefs, analyze the dependence of regime characteristics on geometrical and physical parameters (landslide embedding, its length and thickness, relative density and friction coefficient). It is shown that the character of landslide motion along the irregular slope and surface wave pattern generated by this motion essentially differ from that on the uniform slope.

The modeling of surface waves, generated by the motion of a landslide was made in the framework of the nonlinear model of shallow water over a non stationary bottom. The modified finite-difference MacCormack scheme on a uniform computational grid was utilized [3].

## 2 Set-up of Problem

The mathematical set-up is similar to the one presented at the paper of Chubarov L.B., Khakimzyanov G.S. and Shokina N. published at this book, and, therefore, will be skipped here, as well as the law of landslide motion be in use, whose derivation is also given in details at that work. Only model reliefs and the form of landslide will be described below, as they are different from that used in the work noted.

### 2.1 Model Reliefs

Two reliefs were considered to study the influence of bottom irregularity on the surface waves, generated by the motion of underwater landslide. The first one is the digitized vertical section of Mediterranean coast of Israel in the direction normal to the coastal line near Hadera city. Its minimal depth in the coastal zone was 2 m (but it was enlarged to 20 meters to keep full depth positive during the whole period of calculations), and the maximal depth in the deep-water zone was 1450 m. It consisted of the long shelf zone with slope angle about 1 degree, the slope with incline of up to 7 degrees and gentle deep-water slope with incline no more than 2 degrees.

The second relief was the piece-wise linear approximation of the first one and consisted of the flat bottom with depth 20 m and length 3200 m, uniform slope with inclination of 2 angles, and flat bottom with depth 1400 m and length 27300 m. With given parameters the linear slope had the inclination that is equal to the mean inclination of the "real" relief, and had the same depth 535 m at the point of the initial position of the landslide centre of mass ( $x = 17900$  m). The total length of both water basins was 70000 m.

To fix the results of calculations 2 virtual gages were used: A – on the "shore" ( $x = 0$  m), and B – in the deep-water zone ( $x = 60000$  m).

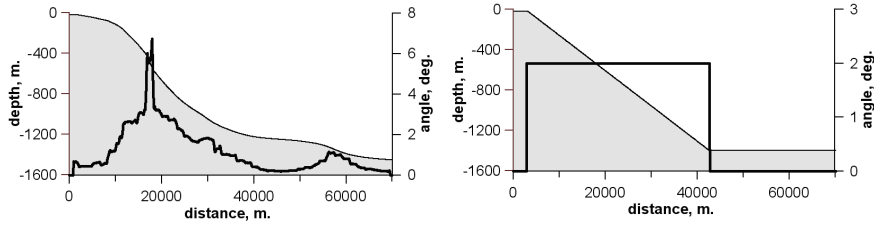


**Fig. 1** Characteristics of model bottom reliefs used in numerical experiments: depth (filled contour, axe is at the left) and slope angle (fat line, axe is at the right): on the left – "real" slope, on the right – linear one

## 2.2 Model Landslide

The shape of the model landslide, which was used in computations, is described by the formula, that is similar to that proposed in [11]:

$$h_{sl}(x,t) = T \frac{[1 + \tanh\left(\frac{(x-x_1(t))^2}{p}\right)][1 - \tanh\left(\frac{(x-x_2(t))^2}{p}\right)]}{[1 + \tanh(1)][1 - \tanh(-1)]},$$

where  $x_1(t) = x_c(t) - \frac{p}{2}$ ,  $x_2(t) = x_c(t) + \frac{p}{2}$ ,  $x_c(t)$  is the  $x$ -coordinate of the landslide mass centre.

The maximum landslide thickness  $T$  was equal to 25 m, parameter  $p$ , that determine landslide length  $b$ , was equal to 2500 m (and then  $b$ , determined on 10% of maximal landslide thickness, was equal to 5000 m). At the start time the landslide mass centre was at the point of maximum inclination of "real" relief  $x_c = 17900$  m, that corresponds to the initial embedding of 535 m.

## 3 Computational Results

Computational experiments were carried out using the simple effective finite-difference scheme, built on the base of MacCormack scheme of the second order of approximation, on the uniform computational grid. The time step was calculated from the stability condition so that Courant number was equal to 0.9. The total number of computational grid points was equal to 1401.

The following parameter values were used in calculations by default: relative density  $\gamma = 1.5$ , added mass coefficient  $C_w = 1.0$ , hydrodynamic drag coefficient  $C_d = 1.0$ , friction angle  $\theta_* = 1^\circ$ .

### 3.1 Dependence on Friction Angle

To study the influence of the friction angle  $\theta_*$  on the body motion and on the characteristics of waves generated, the following values of  $\theta_*$  were used: for linear slope – 0.0, 0.5, 1.0 and 1.5 degrees, and for "real" one – 0.0, 1.0, 2.0 and 3.0 degrees.

Analysis of graphs, which demonstrate the dependence of landslide velocity on the body position on the slope, as well as dependence of landslide acceleration on the time, shows that as friction increases, the distance gone by the body and its velocity both decrease. The picture for acceleration differs slightly: its positive values during the acceleration also have evident inverse dependence on friction angle, but its negative ones do almost not depend on the friction angle.

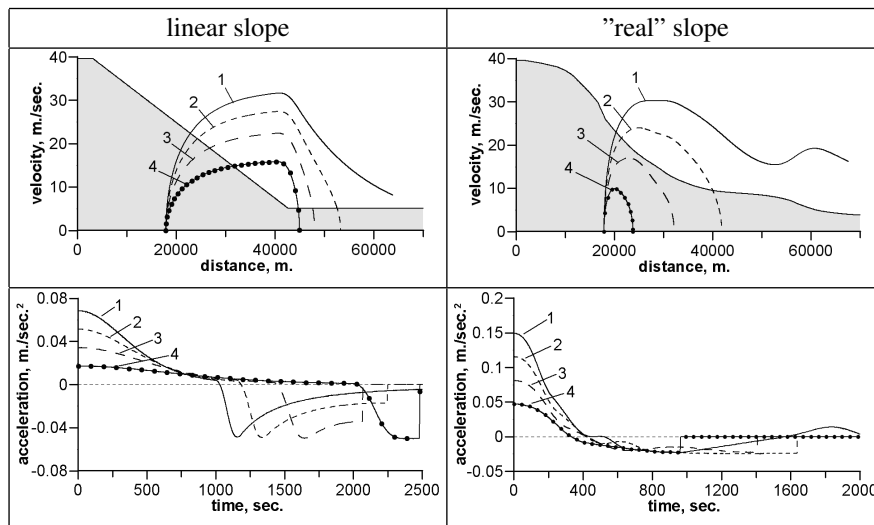


**Fig. 2** Characteristics of laws of landslide motion for different values of friction angle  $\theta_*$ . For linear slope: (1) – 0.0°, (2) – 0.5°, (3) – 1.0°, (4) – 1.5°; for "real" one: (1) – 0.0°, (2) – 1.0°, (3) – 2.0°, (4) – 3.0°

Gauge records of free surface elevations generated by underwater landslide are presented below. The depression wave, recorded near the shore the first, arises at the beginning of landslide motion and goes to the shallow water zone, against the direction of body motion. Its amplitude linearly depends on the initial acceleration, that is seen in big difference between fixed negative amplitudes on gauge A. The first positive wave, registered near the shore, is generated when two negative waves (one is the mentioned above after its reflection off the wall and the second one is the negative wave that goes right over the moving landslide) move over the slope to the zone with larger depths. On the linear slope this wave is seen clearly and its amplitude inversely depends on the friction angle. The second positive wave arises

when the body deaccelerates, and terminates after body finally stops its moving. The amplitude of this wave directly depends on the absolute value of body acceleration just before the stop, therefore this amplitude is the biggest for the widest friction angle.

On the "real" slope the process of deceleration goes faster, therefore both positive waves almost merge, especially for wide friction angle. Here deceleration takes place on different depths: for wider  $\theta_*$  this depth is smaller and it makes the amplitude of generated wave bigger. As a result, the maximum amplitude of positive wave is the same for all  $\theta_*$ , its length is smaller for wider  $\theta_*$  though.

Waves that propagate to the deep-water zone suffer similar changes, when the friction angle varies.

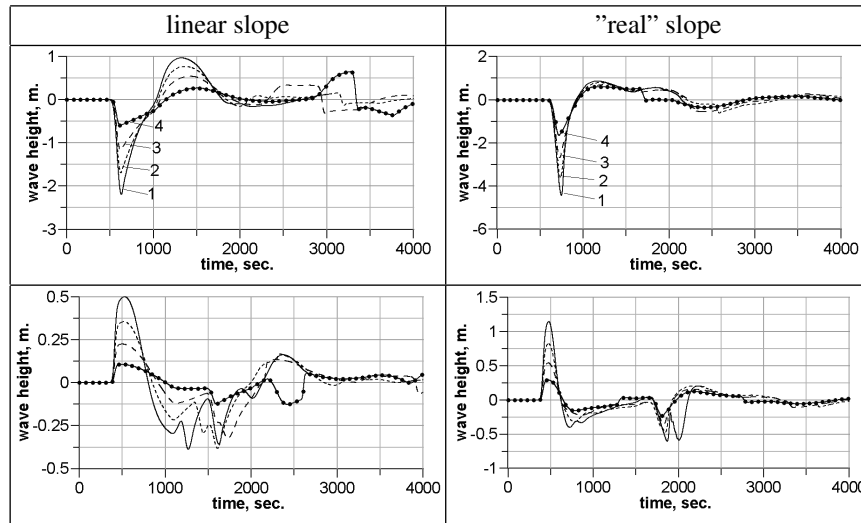


**Fig. 3** Gauge records for different friction angles: top row – gauge A, bottom row – gauge B. For linear slope: (1) –  $0.0^\circ$ , (2) –  $0.5^\circ$ , (3) –  $1.0^\circ$ , (4) –  $1.5^\circ$ ; for "real" one: (1) –  $0.0^\circ$ , (2) –  $1.0^\circ$ , (3) –  $2.0^\circ$ , (4) –  $3.0^\circ$

### 3.2 Dependence on Landslide Size

To investigate the influence of the landslide size on the characteristics of wave regime, the computations with following length and thickness were carried out:  $b = 5000$  m,  $T = 25$  m (reference landslide),  $b = 5000$  m,  $T = 50$  m (double thickness);  $b = 10000$  m,  $T = 25$  m (double length).

As we see on Fig. 4, the law of landslide motion doesn't depend on body's thickness, while varying of it's length appears differently on different slopes. On the one hand, it is due to the specificity of parameter occurrence in the formula of motion

law, and, on the other hand, due to the fact that as body length increases, it occupies new parts of the slope with other inclination. On the "real" slope this effect implies from the very beginning of the motion, and for the linear one – during landslide transition from the inclined part of the slope to the flat one. Thus, on the linear slope initial acceleration doesn't depend on the length of the body, and its maximal negative value is a little less for bigger length, as the left side of the body lays on the slope for a longer time. On the curvilinear slope both initial acceleration and maximum negative one are smaller for bigger length. The maximum velocity is smaller for longer body on both reliefs.

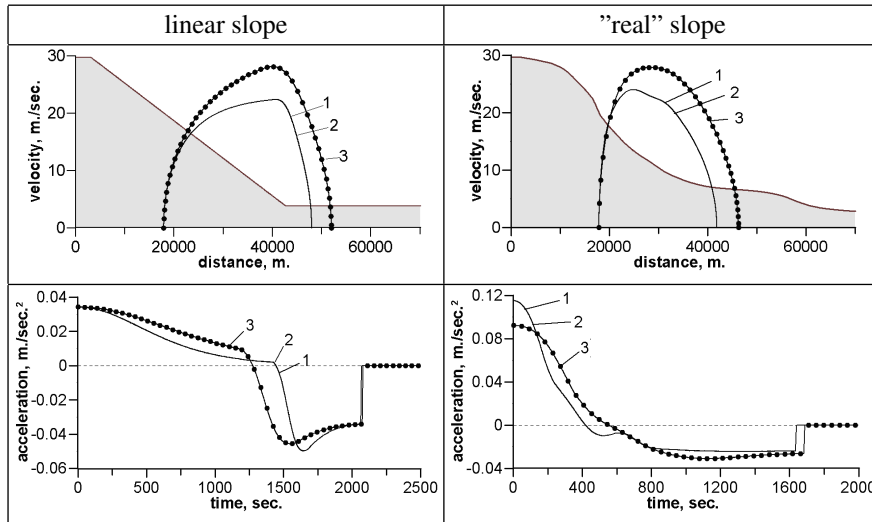


**Fig. 4** Characteristics of laws of landslide motion for different landslide sizes: (1) – "reference" landslide, (2) – double thickness, (3) – double length

As for the waves generated (Fig. 5), on the linear slope duplication of size appears in similar ways: in corresponding duplication of positive and negative wave amplitudes. On the "real" slope duplication of length appears weaker.

### 3.3 Dependence on Landslide Embedding

To investigate the influence of the initial landslide embedding on the wave generation the following values of initial embedding  $d_c$  were considered: 535, 435, 335 and 235 meters.

On the linear slope, as one should expect, the motion character doesn't depend on embedding, except for the start time of deceleration. As velocities are equal before this deceleration, the stopping point is the same, too. On the curvilinear slope the

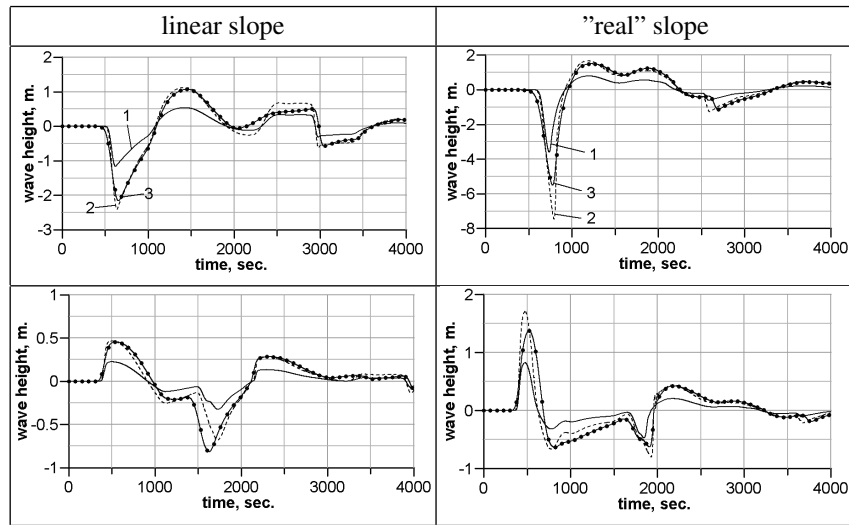


**Fig. 5** Gauge records for different landslide sizes: : top row – gauge A, bottom row – gauge B. (1) – “reference” landslide, (2) – double thickness, (3) – double length

situation is different. Here, the smaller depth, the smaller slope angle and, consequently, the smaller initial acceleration. But, for small  $d_c$ , acceleration grows when body approaches the zone with the largest slope angle and almost reaches the values it has for the bigger embedding. The maximum velocity values increase when  $d_c$  decrease, but the stopping points are almost the same for any  $d_c$ .

The dependence of underwater landslide motion on the initial embedding appears in the wave regime generated in the following way. On the linear slope the amplitude of the first negative wave, propagating towards the shore, increases monotonically with embedding decreasing, but on the “real” one embedding decreasing results in little decreasing of trough amplitude. Amplitudes of the first positive waves near the shore change equally on both slopes: smaller embedding, bigger amplitude. Amplitudes of the second positive waves, generated by body deceleration, are equal for any embedding on both slopes, and this fact is in good correlation with the equality of landslide velocities during deceleration.

### 3.4 Dependence on Landslide Density

The influence of the landslide relative density on the body’s motion and wave formation appears the simplest. The following values of  $\gamma$  were considered here: 1.5, 1.75, 2.0, 2.25.

On both reliefs with relative density increasing maximum values of acceleration and deceleration increase (approximately in two times with density increasing in 1.5



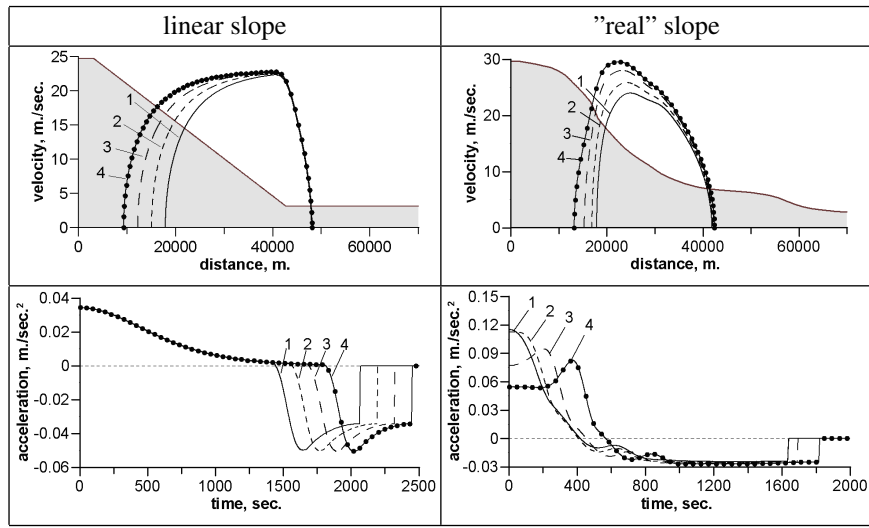


**Fig. 6** Characteristics of laws of landslide motion for different landslide embedding  $d_c$ : (1) – 535 m, (2) – 435 m, (3) – 335 m, (4) – 235 m

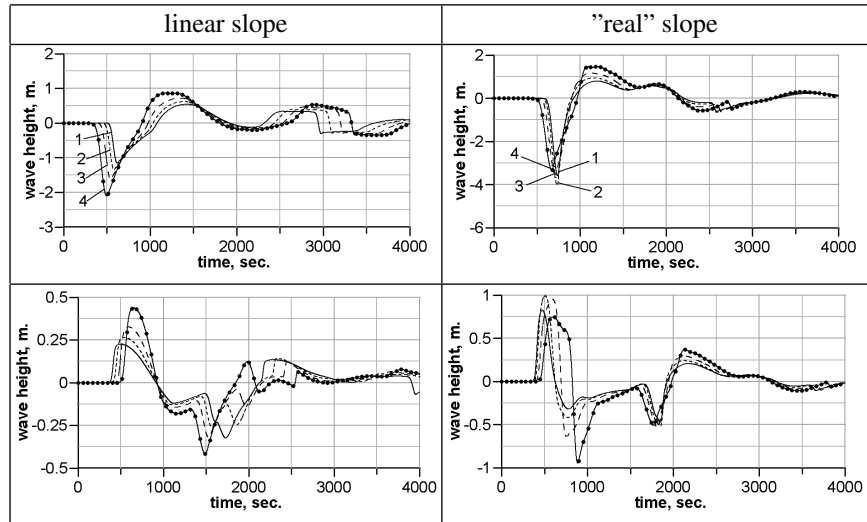


**Fig. 7** Gauge records for different landslide embedding  $d_c$ : top row – gauge A, bottom row – gauge B. (1) – 535 m, (2) – 435 m, (3) – 335 m, (4) – 235 m

times), as well as body velocity (in 1.5 times); the duration of motion is in inverse dependence, and the stopping point doesn't change almost.

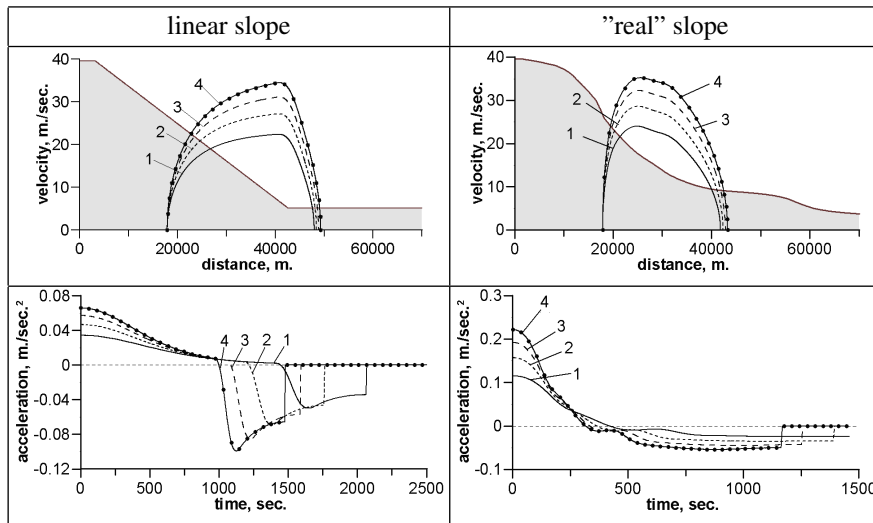


**Fig. 8** Characteristics of laws of landslide motion for different relative density  $\gamma$ : (1) – 1.5, (2) – 1.75, (3) – 2.0, (4) – 2.25

The monotonicity of landslide motion dependence on relative density transmits to the characteristics of wave formation, registered by both gauges. With increase of  $\gamma$ , amplitudes of positive and negative waves increase monotonically, too.

## 4 Conclusions

The results, presented in the article, reflect transition in the study of landslide mechanism of surface waves generation from the simplest linear slopes to the curvilinear "real" ones.

The computational experiments demonstrated the features of influence of landslide size, initial embedding, relative density and friction coefficient over different bottom reliefs. It is shown, that bottom curvilinearity influences essentially in some cases on the character of wave regime dependence on parameters mentioned above.

The features of wave regimes, generated by the landslide motion down the "real" slope, are determined mainly by the taking account of this "reality" in the landslide motion law.

So, variation of the initial landslide embedding results in the variation of angle of the slope, the landslide is situated on, that, in turn, changes the initial acceleration. As a result, for the linear slope the smaller embedding means the bigger wave ampli-

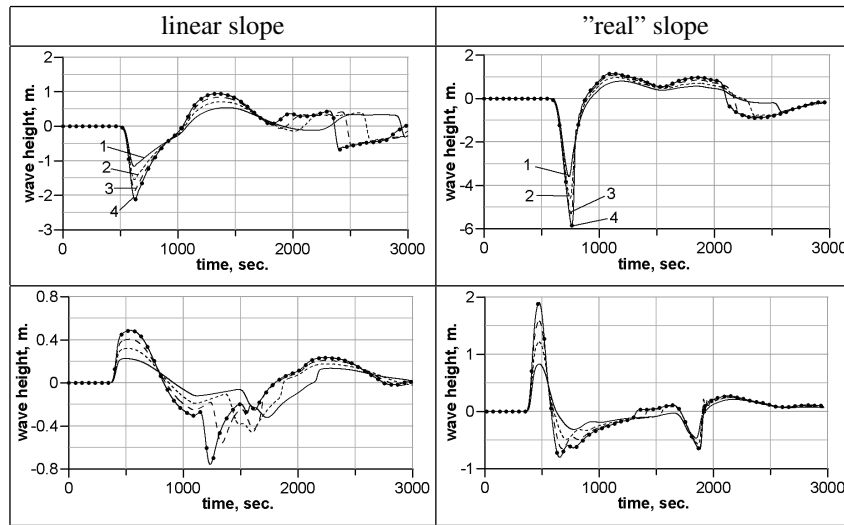


**Fig. 9** Gauge records for different relative density  $\gamma$ : top row – gauge A, bottom row – gauge B. (1) – 1.5, (2) – 1.75, (3) – 2.0, (4) – 2.25

tude, but for the "real" one the most "dangerous" landslide is situated not certainly near the shore.

When landslide length varies, the mean slope angle under the landslide varies too, that has an additional effect on the wave formation.

When the friction force and relative density vary, the characteristics of wave formation change in the same manner over model linear and "real" slopes. Note also, that the friction coefficient is the only considered parameter, which determines the landslide stopping point.

**Acknowledgements** The work was supported by the Russian Foundation for Basic Research (grants 09-05-00294, 06-05-72014) and the Program of Federal Support for Scientific Schools of Russian Federation (931.2008.9).

## References

1. Chubarov, L.B., Eletsii, S.V., Fedotova, Z.I., Khakimzyanov, G.S.: Simulation of surface waves generation by an underwater landslide. *Rus. J. Numer. Anal. Math. Model.* **20**(5), pp. 425–437 (2005)
2. Eletsii, S.V., Maiorov, Yu.B., Maksimov, V.V., Nudner, I.S., Fedotova, Z.I., Khazhoyan, M.G., Khakimzyanov, G. S., Chubarov, L. B.: Simulation of surface waves generation by a moving part of the bottom down the coastal slope. *Comput. Technologies* **9**, Special issue, Part 2, pp. 194–206 (2004) (in Russian)
3. Fedotova, Z.I.: On application of the MacCormack difference scheme for problems of long-wave hydrodynamics. *Comput. Technologies* **11**, Special issue, Part 2, pp. 53–63 (2006) (in Russian)

- Russian)
4. Garagash, I.A., Lobkovskij, L.I.: Geometrical estimation of landslide processes and its monitoring on slope of the Black Sea in view of realization of the "Blue flow" project. In: Proceedings of the Sixth International scientific and technical conference "Up-to-date methods and tools of oceanological investigations", Moscow, pp. 5–15 (2000)
  5. Grilli, S.T., Watts, P.: Modeling of waves generated by moving submerged body. Applications to underwater landslide. *Engineering Analysis with boundary elements*. **23**, 645–656 (1999)
  6. Grilli, S.T., Watts, P.: Tsunami generation by submarine mass failure. I: Modeling, experimental validation, and sensitivity analyses. *J. Waterway Port Coast. Ocean Eng.* **131**(6), pp. 283–297 (2005)
  7. Harbitz, C., Pedersen, G.: Model theory and analytical solutions for large water waves due to landslides. In: Preprint Series, Dept. of Mathematics, Univ. of Oslo. No. 4 (1992)
  8. Heinrich, P., Piatanesi, A., Hebert, H.: Numerical modeling of tsunami generation and propagation from submarine slumps: the 1998 Papua New Guinea event. *Geophys. J. Int.* **145**, pp. 97–111 (2001)
  9. Imamura, F., Imteaz, M.M.A.: Long waves in two-layers: governing equations and numerical model. *Sci. Tsunami Hazards* **13**(1), pp. 3–24 (1995)
  10. Jiang, L., LeBlond, P.H.: The coupling of a submarine slide and the surface waves which it generates. *J. Geophys. Research* **97**, No. C8, 12731–12744 (1992)
  11. Lynett, P.J., Liu, P.L.-F.: A numerical study of the runup generated by three-dimensional landslides. *J. Geophys. Research* **110**, No. C03006, doi: 10.1029/2004JC002443 (2005)
  12. Savage, S., Hutter, K.: The motion of a finite mass of granular material down a rough incline. *J. Fluid Mech.* **199**, pp. 177–215 (1989)
  13. Tinti, S., Bortolucci, E., Vannini, C.: A block-based theoretical model suited to gravitational sliding. *Natur. Hazards* **16**, pp. 1–28 (1997)
  14. Watts, P., Imamura, F., Grilli, S.T.: Comparing model simulations of three benchmark tsunami generation cases. *Sci. Tsunami Hazards* **18**(2), pp. 107–123 (2000)